Supplementary Materials for

High Parasite Diversity Accelerates Host Adaptation And Diversification

Authors: A. Betts[1*], C. Gray[2], M. Zelek[1], R.C. MacLean[1+], K.C. King[1+].

Affiliations:

[1]Department of Zoology, University of Oxford, South Parks Road, Oxford OX1 3PS, UK

[2]Department of Life Sciences, Imperial College London, Silwood Park Campus, Ascot, SL5 7PY, UK

*Correspondence to: Alex.Betts@evobio.eu, Kayla.King@zoo.ox.ac.uk

[+] contributed equally

This PDF file includes:

Materials and Methods

Isolates and bacteriophage characteristics

Independent isogenic lineages of Pseudomonas aeruginosa PAO1 (referred to as the ancestors) were prepared from single colonies with a common ancestor and preserved as stocks of approximately 107 CFU/ml at -80°C with 25% glycerol. Five bacteriophage types were used, three from the Podoviridae (PEV2, LUZ19 and LUZ7) and two from the Myoviridae (1411 and LMA2). All five ancestral phage strains were stored as stocks of approximately 108 PFU/ml at 4°C.

Experimental coevolution

Combinations of the five phages (one-phage monocultures, every possible two-phage combination, and a five-phage community alongside a phage-free control) were prepared such that the phages were at an inoculation titre of $5x10^5$ PFU mL^{-1} and within mixed phage communities, each phage type was present in equal densities. These communities were then mixed with *P. aeruginosa* cultured overnight in KB. Each culture was prepared from a separate ancestral colony and used to inoculate each replicate to a starting concentration of $5x10^7$ colony forming units per mL (CFU mL^{-1}). These experiments were conducted in 5 ml round bottom polystyrene test tubes with vented caps (Corning, *Flintshire, UK*) containing 2.5 ml of King's B (KB) culture medium (microcosms). These microcosms were incubated at 37°C and 2250-RPM orbital agitation in a MaxQ 8000 shaker-incubator (Thermo Scientific, *Waltham, MA, USA*). This experiment was designed to include a blocking structure, with three sequential batches each of 40 lineages. Within each batch, replicates were evenly separated across the three levels of phage diversity (One, Two and Five-phage) and the phage three control such that each treatment had 10 replicates per batch. For each replicate, a 50µl sample containing both bacteria and phage were serially transferred to a new microcosm every 24 hours. Each batch underwent ten such transfers. At each transfer, a 500µl sample was taken and stored in 50% glycerol at -80°C for subsequent analysis.

Measuring host and parasite community density

Every 24 hours samples were taken from each replicate to allow hosts and parasites to be enumerated. Samples were serially diluted and plated via a previously used soft KB agar overlay method to allow the counting of individual phage plaque forming units (PFU) on a lawn of susceptible P. aeruginosa PAO1 from which phage population density (PFU/ml) can be estimated. These diluted samples were simultaneously plated on KB agar to display single bacterial colony forming units (CFU/ml) from which bacterial population density was estimated.

Host and parasite community densities (Fig. 1.A) were analysed using separate linear mixed effects models. We fitted the maximal model with parasite diversity and transfer as interacting fixed effects, and batch, parasite community and replicate as nested random effects. The model was simplified using stepwise model simplification based on AIC. A 2-parameter autocorrelation-moving average correlation structure was built in to the host density model. Post-hoc contrasts were performed using Tukey HSD tests**.**

Measuring parasite infectivity and host resistance

Using a sterile 1 µL inoculation loop, coevolved populations were streaked out onto KB agar. These plates were then placed in a static incubator overnight at 37ºC to allow the growth of individual colonies. Some such colonies were picked with another loop and similarly streaked out and incubated to present single colonies which enables the isolation of phage free, isogenic bacterial populations from the evolved communities. Isolates from each

replicate were used to inoculate individual microcosms incubated for 24 hours. Subsequently a 100 μL sample from each microcosm was mixed with 2.9 mL of molten KB agar (0.75% agar) and spread evenly over the surface of a KB agar (1.5% agar) plate. These soft agar lawns were then inoculated with 4 μL droplets of purified phage, which were allowed to dry, and then incubated for 24 hours. This period allowed the formation of zones of inhibition, which indicated susceptibility or resistance. Droplets which produced with no visible inhibition were scored as resistant (=1), those with some visible inhibition were scored as partially resistant (=0.5), and those with complete inhibition were scored as susceptible (=0). These data were then analysed as the proportion of clones that were resistant or susceptible to a given phage isolate.

Time shift assays: Detecting coevolution between bacteria and phages

A time-shift assay approach enabled the detection of adaptations and counter-adaptations that coevolved during the serial transfer experiment. Bacterial resistance was measured against phage from the same lineage (sympatric), isolated from past, present and future transfers, Likewise, the infectivity of phage was measured on sympatric bacteria from past, present and future transfers. Escalating coevolutionary arms races between hosts and parasites are defined by successive increases in resistance and infectivity. Deviations in linearity, especially those that give rise to local minima or maxima of infectivity and resistance, indicate fluctuating selection dynamics as with the frequency-dependent selection dynamics that underlie Red Queen coevolution. A total of 13,500 combinations of coevolved bacterial genotypes and phage communities were assayed during the time-shift comparing the resistance of bacteria from 24, 120 and 240 hours to the phage communities with which they had coevolved from 10 time points, every 24 hours between 24 and 240 hours. These data were categorised first by the diversity of phage with which they were coevolved and second by whether the contrast combined a bacterial genotype with its contemporary phage community, phage from its past or phage from its future. These data were then analysed in a linear mixed effects model in R (*50*) with bacterial genotype nested within replicate, within phage diversity, within batch as random effects and phage diversity crossed with phage time origin as fixed effects.

Genome resequencing analysis

Whole community DNA extractions were performed on 91 samples for sequencing. Three ancestral *P. aeruginosa* clones and 14 whole populations from the phage-free control were sequenced to enable the identification of mutations resulting from laboratory adaptation and any differences in the ancestor from the published reference sequence (NC_002516.2). In total, 15 one-phage, 10 two-phage and 12 five-phage replicates were sampled longitudinally at two time points (5 days and 10 days) so that allele frequency changes within populations could be easily observed. A subsample of these populations which included the phage PEV2 were analysed to confirm molecular evolution in the bacteriophage. PEV2 was chosen as its reference genome was most recently sequenced and is comparatively well annotated for a bacteriophage genome, all of the phages used here have published reference genomes (KU948710.1, NC_013691, NC_010326, NC_011703 & NC_011166) but the vast majority of genes are of unknown function, for example; all but two of the genes in the parasite 14-1 are hypothetical proteins. In the case of PEV2, more than one gene relating to tail fibre production has been identified and tail fibres are known to be an important structure under selection during antagonistic coevolution between phage and bacteria. The parasites used here all have sequenced reference genomes against which any sequenced reads could be mapped (KU948710.1, NC_013691, NC_010326, NC_011703 & NC_011166). We used coverage data from the Phage mappings to estimate the relative composition of each

community at different time points by using the number of mapped reads as a proxy for relative abundance. We selected 2 PEV2 low diversity replicates, 4 medium diversity replicates (one each in which PEV2 coexisted with the other four phage types) and six high diversity replicates. Each of these replicates was analysed at both the mid and endpoint of the experiments.

Whole community DNA extractions were performed on 1ml of culture using a DNeasy Blood and Tissue kit (Qiagen, Inc., Chatworth, California, USA), quantified using the QuantiFluor dsDNA system (Promega, Madison, WI, USA) and the salt ratio verified by Nano Drop (Thermo Scientific, Waltham, MA, USA). Whole genome sequencing services were provided by the Wellcome Trust Centre for Human Genetics (Oxford, UK) using the Illumina HiSeq platform with 150 bp paired-end reads. All mapping and variant calling was performed using CLC genomics Workbench (CLC Bio). First, 5' or 3' ends were trimmed if the Phred quality score was less than 20. Reads were discarded if they were shorter than 50 bp after trimming or if more than 2 bases were ambiguous. Filtered reads were then mapped to the *P. aeruginosa* PA01 reference genome or the Pseudomonas phage PEV2 reference genome. Mapped reads were then processed to increase the quality of the variant calling; duplicated reads were discarded and reads around indels were locally realigned. A Neighbourhood Quality Standard model was then applied to detect single nucleotide polymorphisms and a separate model was used concurrently to detect deletion/insertion polymorphisms. Variants were then filtered to remove any also present in the three sequenced ancestral clones or one ancestral phage population, thus ensuring that all reported SNPs are certain to have arisen during the experiment, not before. Finally, variants in the host samples were annotated using the Pseudomonas database (*51*) whereas the parasite variants were annotated using the reference sequence as no larger database exists for these parasites.

Detecting genetic signature of coevolution using Host and Parasite SNPS

Previously published data has shown that host LPS genes and parasite tail fibre genes can be the focus of antagonistic coevolution (*24*). Using the SNP data collected for both the hosts and parasites we computed a gene interaction matrix for each of the subsampled replicates containing PEV2. For every possible host gene – parasite gene combination, we calculated the number of communities in which mutations in those genes co-occurred. To visualize the relationship the frequency at which a particular gene pair co-occurred was then used to weight the interactions in a host-parasite gene interaction network produced using bipartite in R showing every possible gene combination across all replicates. In the majority of cases (69%), mutations in particular host and parasite genes only co-occurred in a single replicate. By contrast, the two most common gene co-occurrences were between a parasite tail fibre gene (gp52) and either of two host LPS biosynthesis genes (wzy or mig8). These data strongly support antagonistic coevolution driven by mutations in parasite tail fiber genes and host LPS genes.

Detecting genomic signatures of strong directional selection

We used PoPoolation 2 (*52*) to calculate the per locus F_{ST} between each 10 day coevolved population and one of the three isogenic sequenced ancestors. The mapped genomes were sorted and synchronised using SAMtools (*53*). The FST was then calculated for every SNP genomewide using the FST-sliding tool of Population 2. The majority of the 6.3 million loci were not under strong selection in this experiment and produced very low FST values. All values <0.05 were excluded and with the remaining data (mean 0.174 s.d. = 0.164) we calculated 3 standard deviations above the mean to give a conservative threshold FST of 0.67, all values higher than this were taken to be indicators of strong directional

selection driving alleles towards fixation. The number of mutations with signatures of strong directional selection was compared between treatments with a chi-squared test.

Determining effects of parasite diversity on evolutionary rates

The Euclidean genetic differences (the square root of pairwise differences) between each coevolved population ancestor was calculated using the frequency of detected variants. Indels varied in size but were each counted as just a single mutation. Host mutations with a frequency of <5% and parasite mutations with a frequency of <10% were not included to optimize the quality of our data sets. A phylogeny was produced on the resultant distance matrix using the library APE (*54*) in R (*50*). The significance of the differences in genetic distances between treatments was compared by ANOVA and post hoc contrasts were performed using Tukey HSD tests.

The Euclidean genetic distances between each coevolved host population were investigated by nMDS ordination and ANOSIM which partitions diversity within and between treatments and computes a value or $R \approx 0$ when there is no difference. Secondly, the genetic distances between each coevolved host population within each diversity treatment were analysed by ANOVA followed by post hoc Tukey HSD tests. Within population diversity was estimated with Shannon's diversity index calculated from the SNP data.

We also performed the test for transgressive overyielding (D_{max} (*55*)) e.g. is host evolutionary rate greater with a community of parasites A, B & C than with monocultures of either A, B or C. This confirmed if our diversity effect was due to diverse communities being more likely to contain phages which drive rapid evolution rather than a positive interaction between phages in communities accelerating coevolution. We calculated D_{max} using the genetic distances from the high parasite diversity treatment and the genetic distances of each of the parasites in monoculture. One-sample t-tests were performed with a Bonferroni correction to test whether each phage had a D_{max} significantly greater than zero.

Supplementary Text

Analysis of ecological data

Parasite diversity significantly affected host population density ($F_{3,45} = 6.59$, $P < 0.001$). The highest host densities were achieved with high parasite diversity, but host densities increased over time regardless of parasite diversity ($F_{1,1079} = 160.74$, $P < 0.001$). We observed no time-dependent relationship with the parasite community densities. Indeed, the only significant factor explaining parasite densities was parasite diversity ($F_{2,43} = 6.1$, $P < 0.01$) with the high parasite diversity treatment reaching the highest parasite density (Post-hoc Tukey test $P < 0.05$).

Accelerated resistance evolution could have important ecological consequences as parasites require susceptible hosts to complete their lifecycles (*56*). In the absence of any evolutionary change, we would expect parasite populations to grow with host populations. Our observation that parasite densities were stable over time despite simultaneously increasing host densities suggests feedbacks between evolutionary and ecological dynamics (*19*) and confirms the evolution of host resistance. That parasite densities do not subsequently decrease in the face of increasing resistance (and dilution into fresh media every 24 hours) agrees with our time shift results and could be explained by a quick coevolutionary response from the parasites allowing them to infect the new host genotypes (*20*).

Analysis of time-shift data

We observed that parasite diversity significantly increased the magnitude of resistance and infectivity evolution over time ($F_{2,85}$ =9.7, P < 0.001) with the low parasite diversity treatment selecting for the least resistance and most infectivity; significantly different to the intermediate (Post-hoc Tukey test P < 0.05) and high parasite diversity treatments (Post-hoc Tukey test P < 0.001). The data also show significant change in the ability of parasites to infect hosts over time ($F_{2,13044}$ =1766.21, P < 0.0001). Within each level of parasite diversity, resistance was always lowest to parasites from the future and highest to parasites from the past (Post-hoc Tukey test P < 0.0001). This pattern is typical of arms race dynamics, commonly seen in in vitro bacteria-phage interactions (*5*, *22*). The significant interaction between parasite diversity and parasite time origin ($F_{4,13044}$ =16.99, P < 0.0001) is largely explained by the differing abilities of parasite communities to overcome evolved host resistance. Interestingly, the resistance of host populations to their contemporary parasite communities were very similar (Post-hoc Tukey test P > 0.2) yet the resistance of the intermediate parasite diversity coevolved hosts to past and future parasites was significantly lower (Post-hoc Tukey test P < 0.05) than the high parasite diversity coevolved hosts. These results suggest a greater ability of the host populations facing high parasite diversity to evolve resistance.

Phage diversity PCR

The presence or absence of the five different phage types at the end of the experiment in the high parasite diversity treatment was confirmed via PCR.

Primers specific to each phage (Table S4.) were designed and tested for potential cross amplification against the *P. aeruginosa* chromosome and the other phage types used here in Geneious 6.06 (Biomatters Ltd. Auckland, NZ). All primer pairs were designed with an amplicon size of 150bp within genes thought to encode the tail fibre proteins of each phage. PCR was performed using GoTaq green Mastermix (Promega, Madison, WI, USA) on whole community DNA extracted 1ml of culture using a DNeasy Blood and Tissue kit (Qiagen, Inc., Chatworth, California, USA).

The number of phage types detected in the samples from the end of the experiment (Fig. S4.) were analysed by ANOVA. In several samples, different phage have fallen below the detection threshold, but not to the extent that our diversity treatments were compromised (ANOVA $F_{2,34}$ =38.73, P < 0.001) the high diversity treatment remains more diverse than the medium (Post-hoc Tukey test P < 0.0001), which is in turn more diverse than the low (Post-hoc Tukey test P < 0.05).

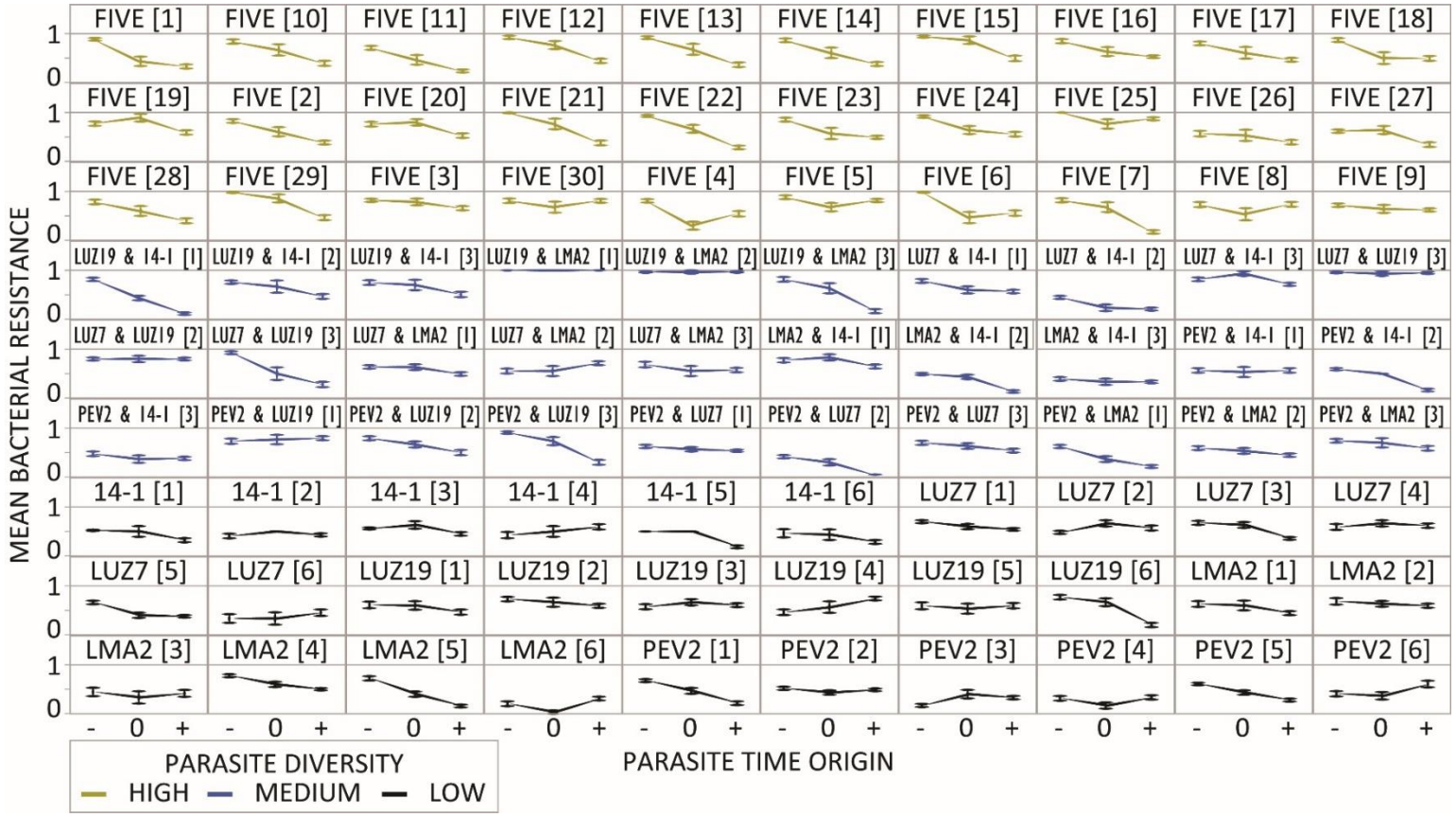

Fig. S1 Coevolutionary trajectories vary between replicates. By comparing the resistance of hosts from multiple time points to parasites from their coevolutionary past, present and future from all levels of parasite diversity (low (black), medium (blue) and high (yellow)), the pattern of phenotypic change in hosts and parasites through time can be summarised. The header for each panel lists the species of parasite present with the replicate number in square brackets. Here, individual communities displayed an incredible diversity of changes in infectivity and resistance over time. Despite this extraordinary complexity, by combining these data with our molecular data we were able to discern the effects of diversity on coevolutionary dynamics (-= parasites from host's past, 0= parasites from host's present, += parasites from host's future. Error bars indicate 1 standard error.

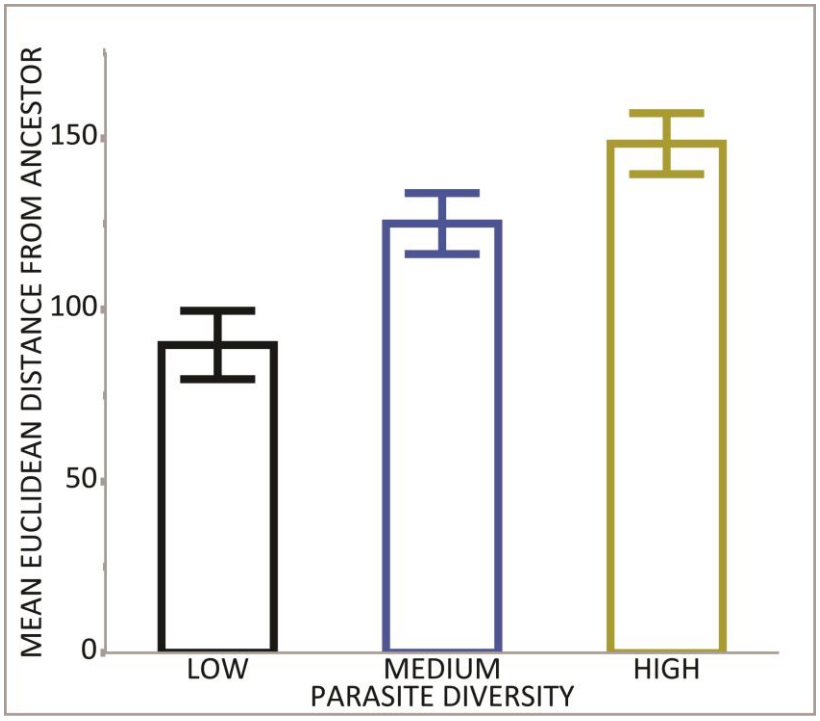

Fig. S2 Parasite diversity drives host evolution. We compared the mean Euclidean distance between the host populations that had coevolved with parasite communities of different diversities (low (black), medium (blue) and high (yellow)). Parasite diversity significantly increased evolved host distance from the ancestor (ANOVA $F_{2,34} = 10.5$, $P < 0.001$). The low diversity populations had the lowest mean distance from the ancestor (Post hoc Tukey test $P < 0.05$). Error bars show 1 standard error.

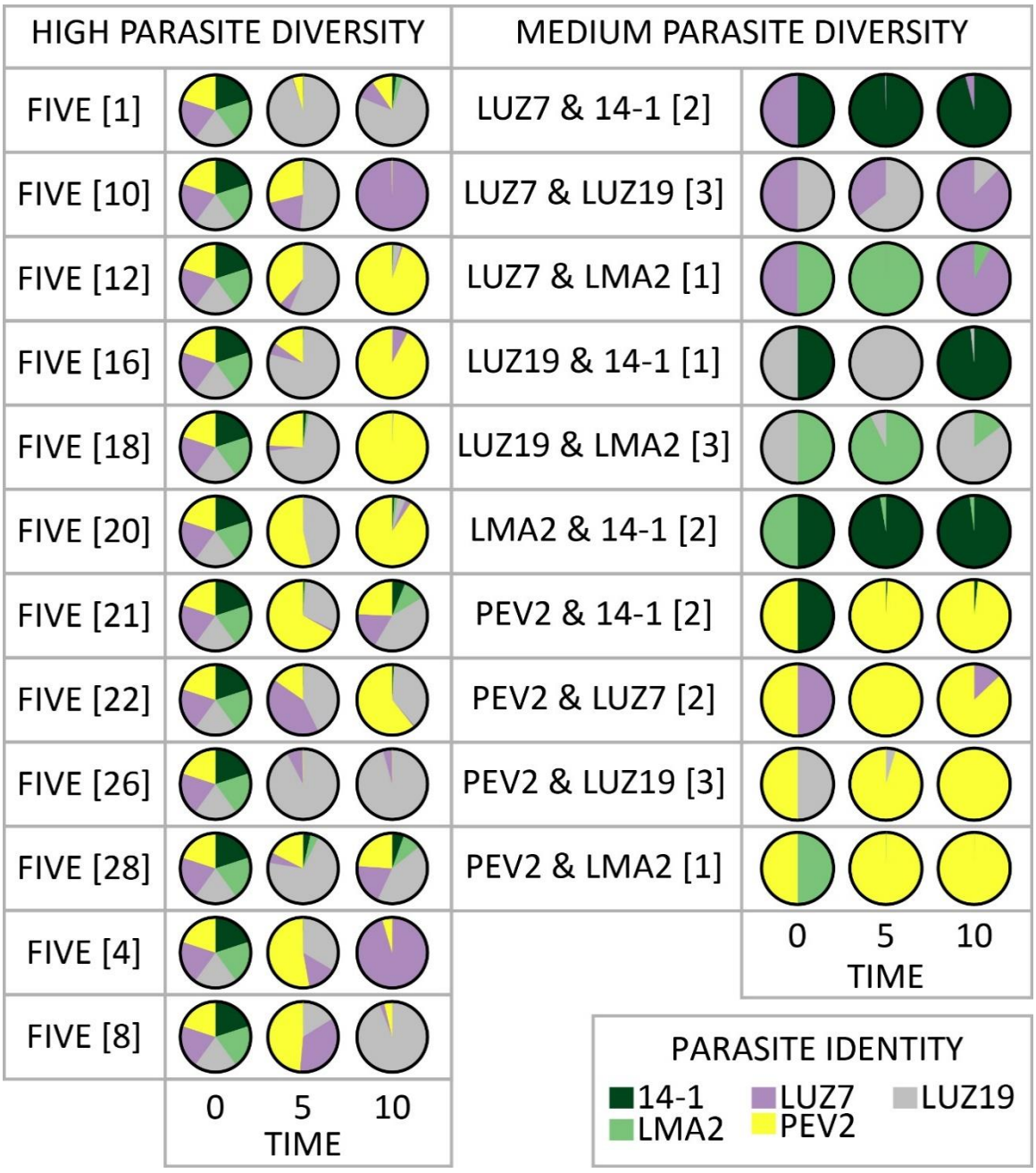

Fig. S3 A time series of parasite community composition. Each panel in this figure contains three pie charts providing snapshots of the relative composition of a parasite community from the start, mid and end-points of the experiment. The starting composition was controlled by our experimental conditions, the composition on days 5 and 10 were estimated using the number of sequencing reads that would map to the relevant genome as a proxy for relative parasite abundance. The figure shows data from the medium and high diversity treatments.

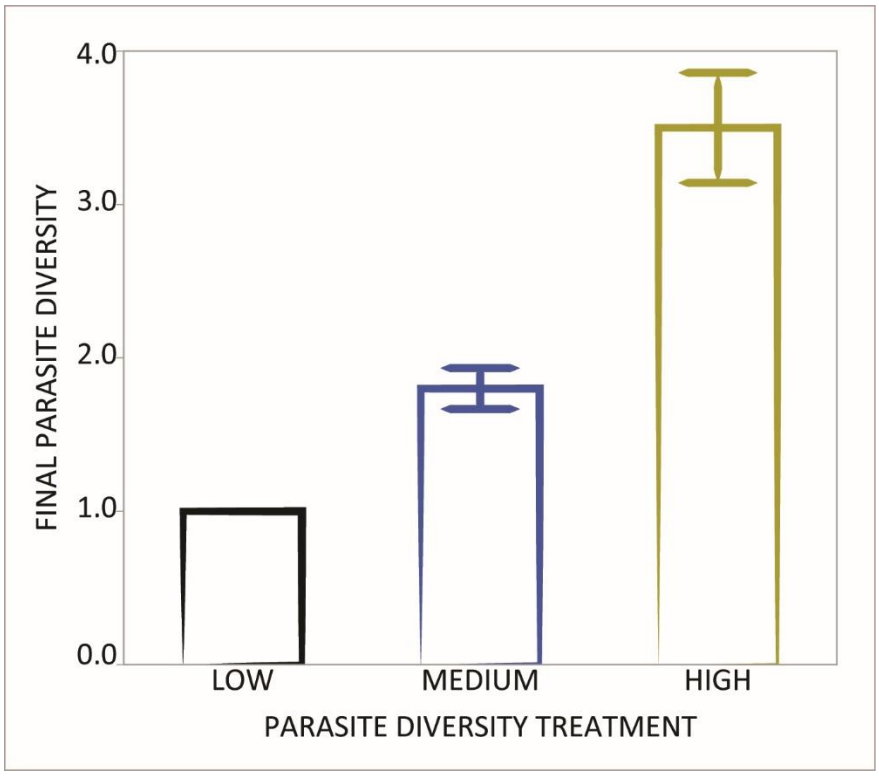

Fig. S4 Changes in parasite community diversity. To test for changes across all levels of parasite diversity (low (black), medium (blue) and high (yellow)) during coevolution we tested for the presence/absence of phage at day 10 of the evolution experiment using PCR on community genomic DNA. Bars show the mean (+/- standard error) number of phage species detected as a function of initial parasite diversity. Phage extinctions occurred in some communities, but not to the extent that our diversity treatments were compromised (ANOVA $F_{2,34}$ =38.73, $P < 0.001$) the high diversity treatment remains more diverse than the medium (Post-hoc Tukey test $P < 0.0001$), which is in turn more diverse than the low (Post-hoc Tukey test $P < 0.05$). Methods: Primers specific to each phage (Table S4.) were designed and tested for potential cross amplification against the *P. aeruginosa* chromosome and the other phage types used here in Geneious 6.06 (Biomatters Ltd. Auckland, NZ). All primer pairs were designed with an amplicon size of 150bp within genes thought to encode the tail fibre proteins of each phage. PCR was performed using GoTaq green Mastermix (Promega, Madison, WI, USA) on whole community DNA extracted 1ml of culture using a DNeasy Blood and Tissue kit (Qiagen, Inc., Chatworth, California, USA).

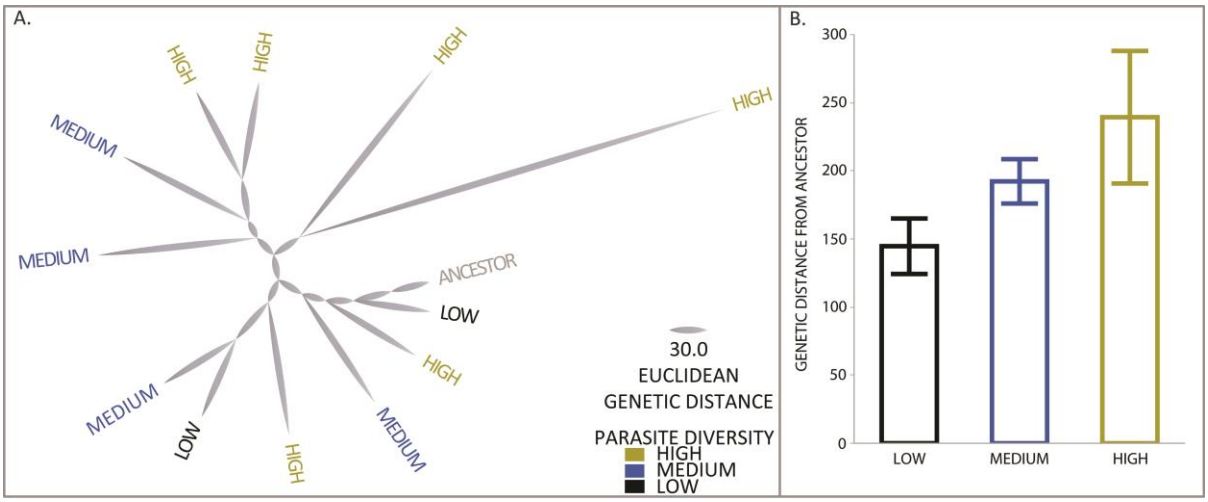

Fig. S5 Parasite diversity does not accelerate parasite evolution. (A) A tree based on Euclidean genetic distance data from our sequenced PEV2 populations from all levels of parasite diversity (low (black), medium (blue) and high (yellow)). This figure was prepared using the same methods as Fig 2(A) in the main manuscript. (B) This figure shows the mean genetic distance from the ancestor, the rate of evolution, in PEV2 across the three treatment levels. It is worth noting that the sample size is smaller here than for the corresponding analysis used to analyse the host data. There was no significant effect of parasite diversity on PEV2 evolutionary rate (ANOVA $F_{2,9} = 14910$, $P = 0.44$).

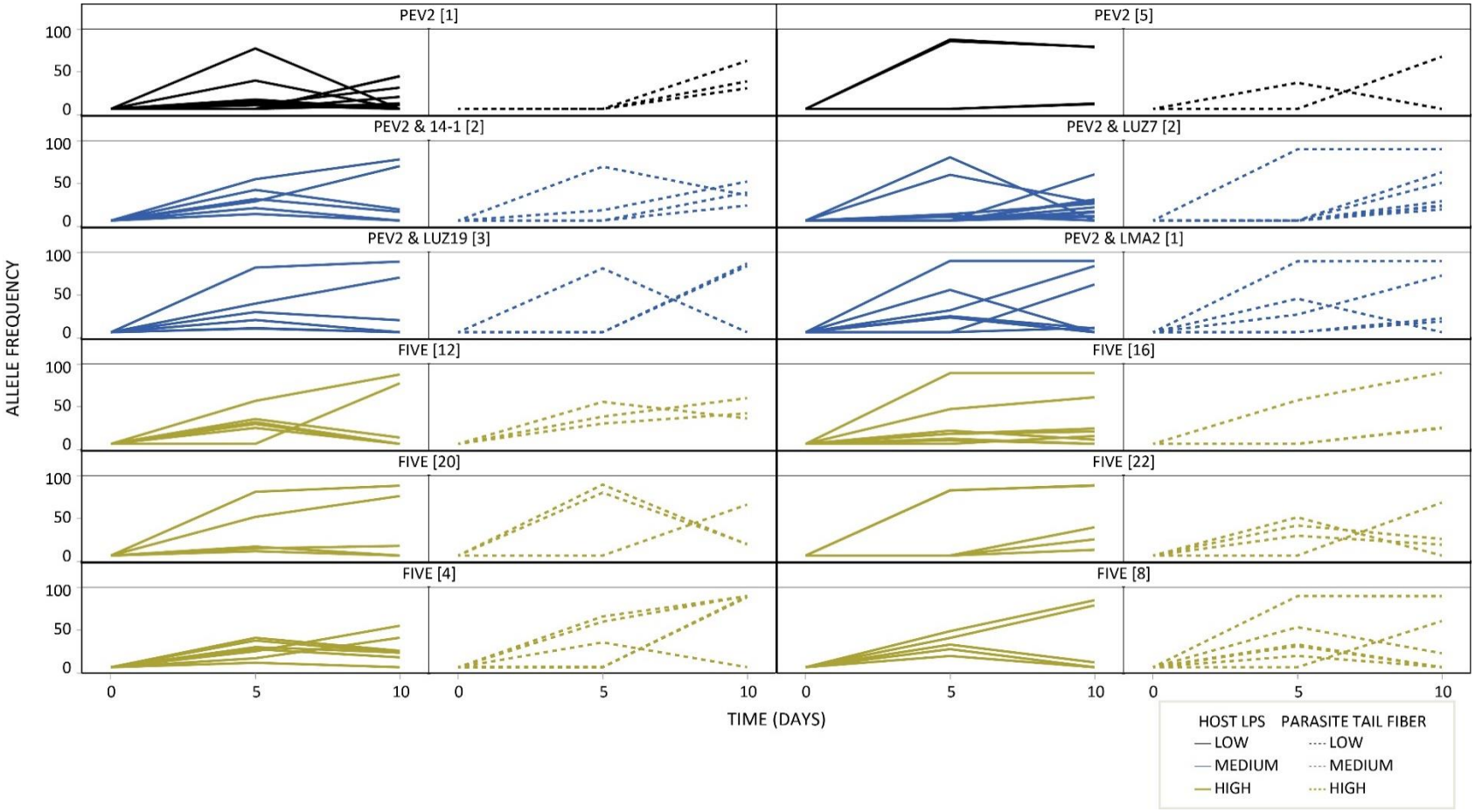

Fig. S6 Genomic evidence for antagonistic coevolution. This figure shows the host LPS biosynthesis allele frequencies (solid lines) alongside the parasite tail fiber allele frequencies (dotted lines) for the phage PEV2 across all levels of parasite diversity (low (black), medium (blue) and high (yellow)). Host LPS serves as the receptor for this parasite and the tail fibers are the means by which the parasite recognizes and binds to its receptor. These data support the phenotypic data which clearly shows increasing parasite infectivity and increasing host resistance over time and conclusively demonstrate antagonistic coevolution at the genomic level.

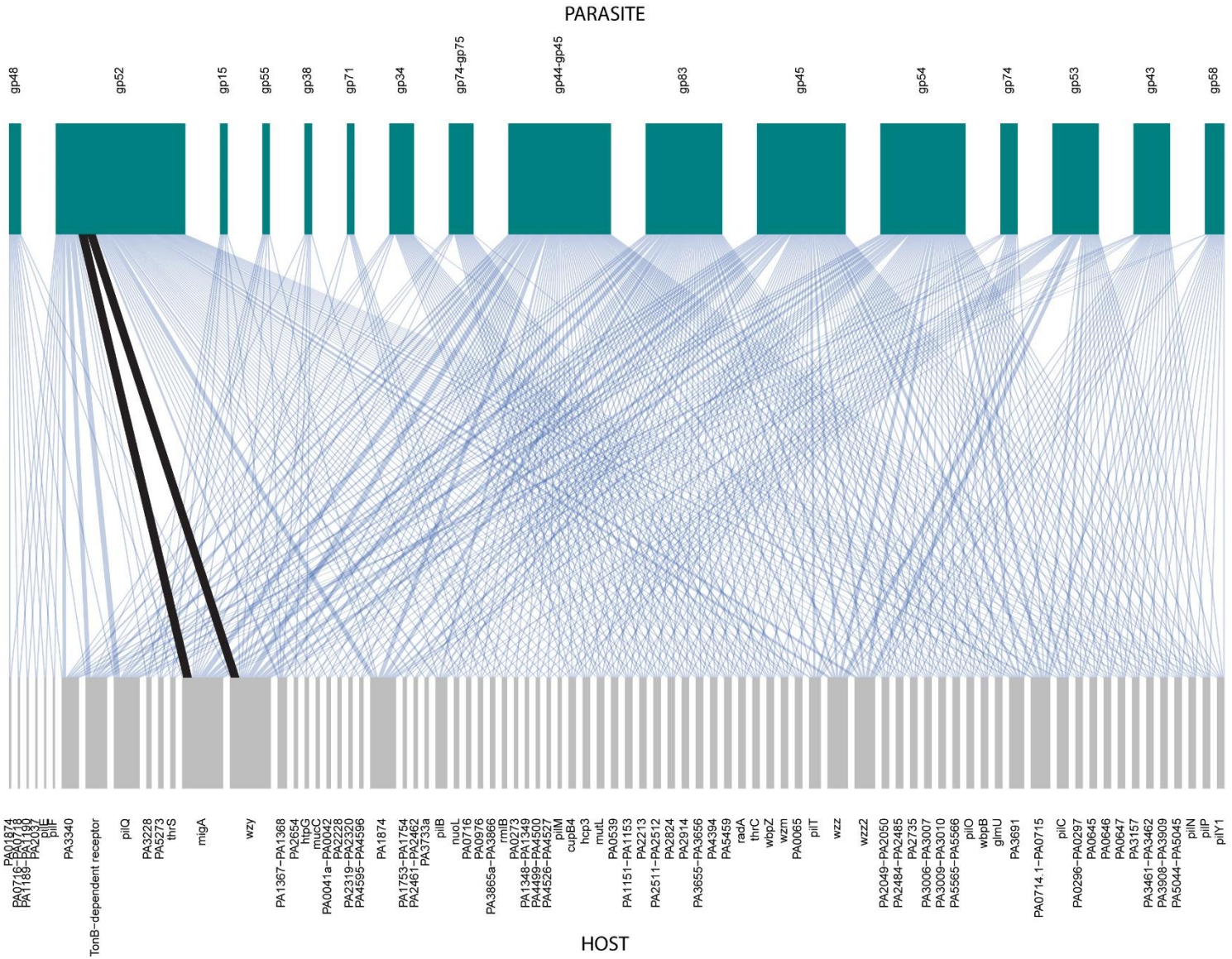
PARASITE
gp48
gp52
gp15
gp55
gp38
gp71
gp34
gp74-gp75
gp44-gp45
gp83
gp45
gp54
gp74
gp53
gp43
gp58
PA0187
PA0716–PA0718
PA1189–PA1190
PA2037
pilE
pilF
PA3340
TonB–dependent receptor
pilQ
PA3228
PA5273
thrS
migA
wzy
PA1367–PA1368
PA2654
htpG
mucC
PA0041a–PA0042
PA2228
PA2319–PA2320
PA4595–PA4596
PA1874
PA1753–PA1754
PA2461–PA2462
PA3733a
pilB
nuoL
PA0716
PA0976
PA3865a–PA3866
rmlB
PA0273
PA1348–PA1349
PA4499–PA4500
PA4526–PA4527
pilM
cupB4
hcp3
mutL
PA0539
PA1151–PA1153
PA2213
PA2511–PA2512
PA2824
PA2914
PA3655–PA3656
PA4394
PA5459
radA
thrC
wbpZ
wzm
PA0065
pilT
wzz
wzz2
PA2049–PA2050
PA2484–PA2485
PA2735
PA3006–PA3007
PA3009–PA3010
PA5565–PA5566
pilO
wbpB
glmU
PA3691
PA0714.1–PA0715
pilC
PA0296–PA0297
PA0645
PA0646
PA0647
PA3157
PA3461–PA3462
PA3908–PA3909
PA5044–PA5045
pilN
pilP
pilY1
HOST

Fig. S7 Genomic evidence for genetic specificity of antagonistic coevolution. A bipartite network plot of host-parasite gene interactions across all treatments where the width of the lines is scaled by the frequency at which that interaction was observed. Previously published data has shown that host LPS genes and parasite tail fibre genes can be the focus of antagonistic coevolution (*24*). Using the SNP data collected for both the hosts and parasites we computed a gene interaction matrix for each of the subsampled replicates containing PEV2. For every possible host gene – parasite gene combination, we calculated the number of communities in which mutations in those genes co-occurred. To visualize the relationship the frequency at which a particular gene pair co-occurred was then used to weight the interactions in a host-parasite gene interaction network produced using bipartite in R showing every possible gene combination across all replicates. When the networks of all possible interactions between coevolved host and parasite genes (intergenic mutations are shown giving the upstream and downstream gene IDs separated by a hyphen) are examined, clear patterns start to emerge. Of the 508 possible pairwise combinations of host (bottom) and parasite (top) genes, 442 occur are unique and only 2 combinations occur in >50% of replicates. When the functions of these genes are examined the data show that in every sequenced community there are mutations in host LPS biosynthesis genes and parasite tail fibers, and by far the most common of these associations was between the host LPS biosynthesis genes (wzy and migA) and the parasite tail fiber protein gene (gp52) which each co-occurred in 8/12 replicates. These interactions are shown in black on the figure. The extreme overrepresentation of these associations supports previously findings in bacteriophage – host coevolution driven by mutations in host LPS biosynthesis genes and parasite tail fibers genes.

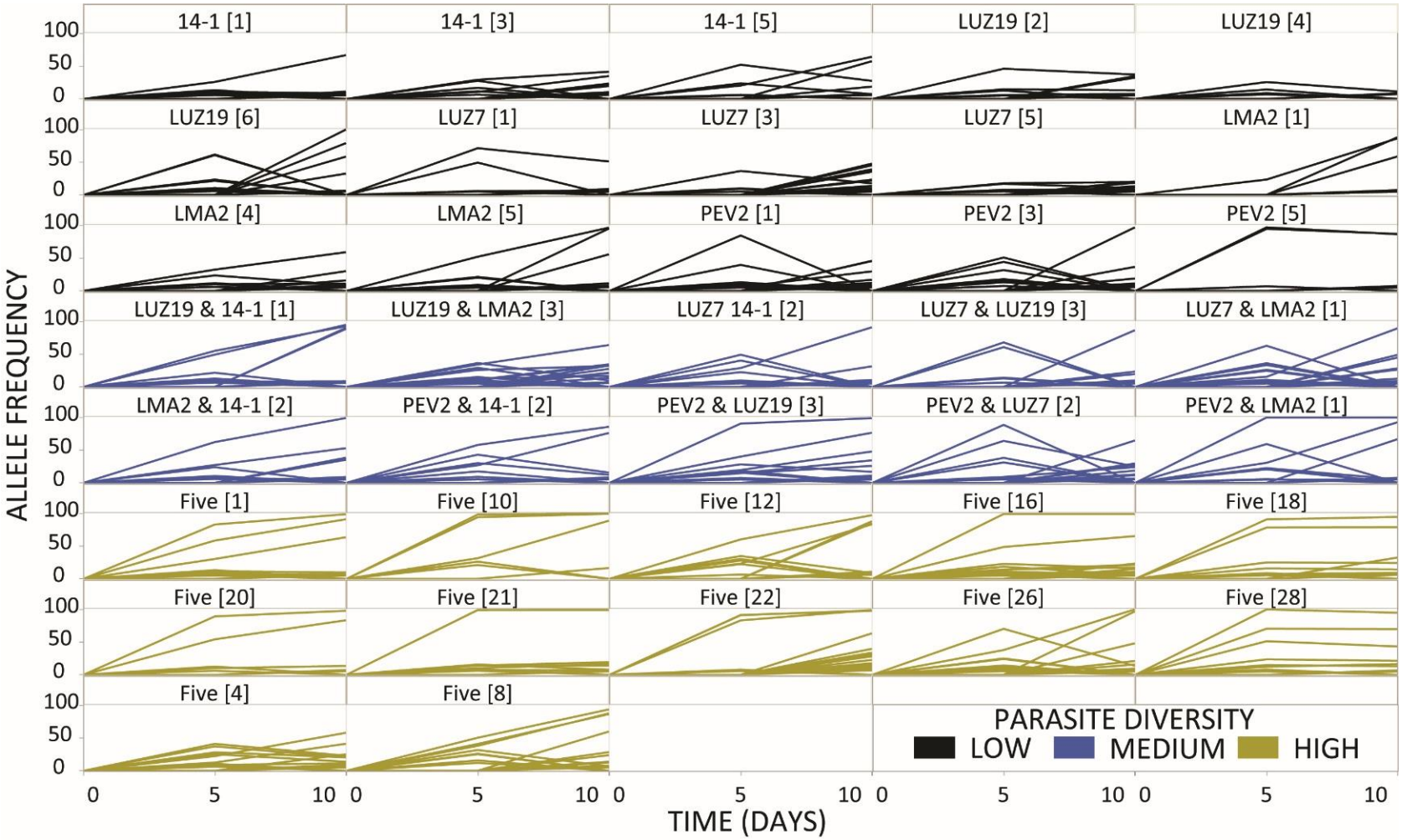

Fig. S8 Parasite diversity encourages harder selective sweeps. The frequency of each observed mutation in each sequenced population from the start, mid and endpoints of the experiments from the low (black), medium (blue) and high (yellow) parasite diversity populations. More alleles reach higher frequencies in the high parasite diversity treatment than in the medium or low.

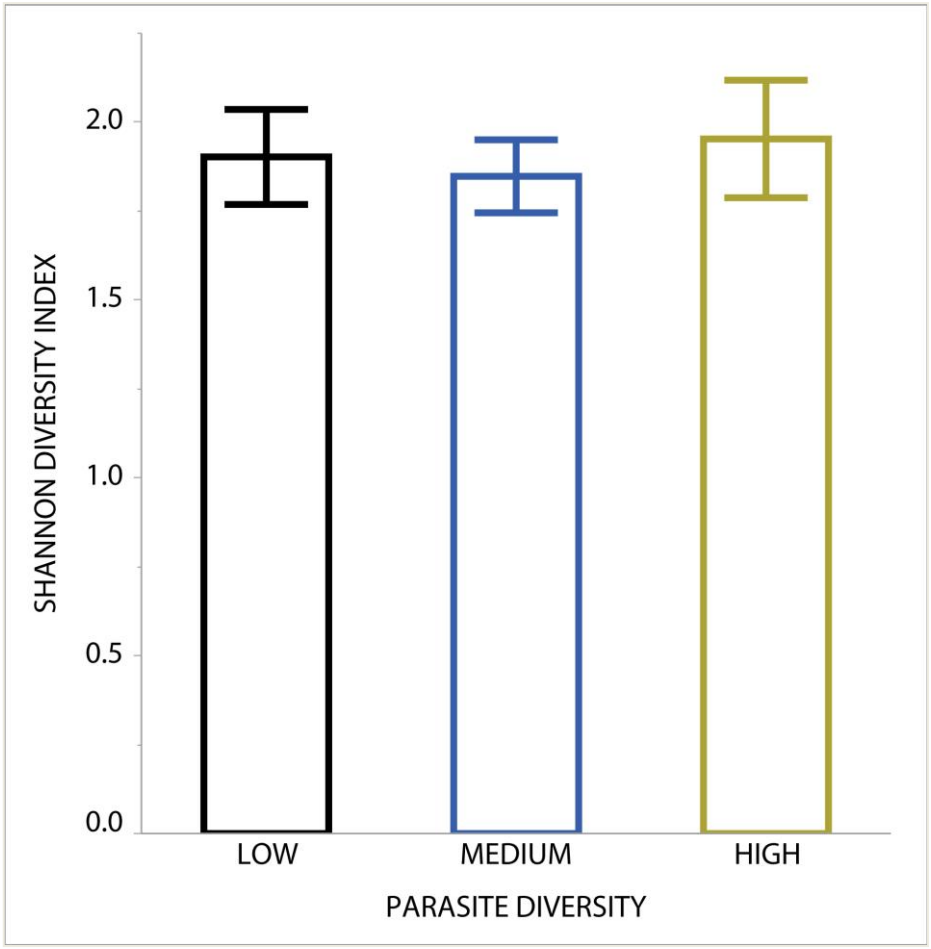

Fig. S9 Parasite diversity does not impact within sample host diversity. Shows the mean within sample diversity as scored on the Shannon Diversity index from SNP frequency data from the low (black), medium (blue) and high (yellow) parasite diversity populations. There was no significant effect of parasite diversity on within sample host diversity (ANOVA $F_{2,34} = 0.06$, $P = 0.88$). Error bars show 1 standard error.

Table S1.

Identities of host genes in which mutations were particularly likely to be detected pooled across all treatments.

Gene Function	Number of mutations	Number of genes mutated	Genes with >10 mutations
LPS Biosynthesis	190	10	PA3154 (*wzy*), PA3160 (*wzz*), PA0938 (*wzz2*) and PA0705 (migA)
Type IV pili formation	69	17	PA5040 (*pilQ*) and PA4526 (*pilB*)
TonB-dependent receptor	55	1	PA2911
Other / unknown / intergenic	368	146	PA1874

Table S2.

Identities of parasite (PEV2) genes in which mutations were particularly likely to be detected pooled across all treatments. The gp71 mutations all occurred in a single sample whereas gp52 was the only gene in which mutations were detected for every sample.

Gene Function	Number of mutations	Number of genes mutated	Genes with ≥10 mutations
Putative tail fiber protein	83	2	gp52
RNA polymerase	10	1	gp71
Other / unknown / intergenic	132	17	gp45, gp53, gp54, gp83 and intergenic gp44-gp45

Table S3.

Shows the number of mutations that reached >10% frequency in each of the five parasites across all sequenced replicates alongside the proportion of these that were non-synonymous.

Phage Type	# Observed mutations	Proportion non-synonymous
14_1	44	0.9
LMA2	6	1.0
LUZ19	158	0.7
LUZ7	52	0.8
PEV2	225	0.8

Table S4.

This table gives details of the phage specific primer pairs used here and the identity of their target regions.

Phage	Gene	Forward Primer	Reverse Primer
PEV2	gp53	TGCCGAAGCATTGGTCAGAT	GACTACACCGACCAGTGGTG
LUZ7	gp056	TGACCACGTACTCGGTGTTG	ACAAGCTGGGCCAGTTCTAC
LUZ19	gp40	ACCCTAGCTGGTCAAGTCCT	CACCAGAGTAGTAGGCTGCC
LMA2	gp38	TACAATCAGCAGCGCATCCA	CCGGAAAGTGTCTGCCAGAT
14-1	gp45	CTTAGCAGCACGACTTGGGA	CTCCCACGTCCCATTCAACA